COMPARATIVE STUDY OF THE SURFACE RADIATION BUDGET AT NY-ÅLESUND, SVALBARD AND SYOWA STATION, ANTARCTICA, 1987

Takashi YAMANOUCHI[1] and Jon Børre ØRBÆK[2]

[1]*National Institute of Polar Research,*
9–10, Kaga 1-chome, Itabashi-ku, Tokyo 173
[2]*Norwegian Polar Institute,*
Middelthunsgate 29, Majorstua, N-0301 Oslo, Norway

Abstract: The surface radiation budget in 1987 at Ny-Ålesund, Svalbard was measured by the Norwegian Polar Institute, and is discussed as a typical radiative regime for the Arctic, at the edge of the seasonal sea ice area. Following the dramatic change of surface albedo between summer and winter, global solar radiation decreases under clear and overcast conditions at the same solar zenith angle. The apparent transmittance defined as the ratio of the global radiation at the surface to the solar insolation at the top of the atmosphere ranges from 40 to 70% before the decrease of albedo; however, it ranges from 20 to 60% after the decrease of albedo. The downward longwave radiation differs considerably between winter and summer. In summer, the downward longwave radiation has a small range and the difference between clear and overcast is small, while cloud amount is very high. In winter, the range of downward longwave radiation is as great as 150 W/m², from about 150 W/m² under clear sky to more than 300 W/m² under overcast sky in some cases. This great variation in winter is due not only to the variation of cloudiness but also to the variation of air mass surrounding Ny-Ålesund. Larger downward longwave radiation with high cloudiness and warmer temperature accompany maritime airmasses; smaller radiation with low cloudiness and colder temerature accompany the Arctic airmass. Normally, polar clouds increase the downward longwave radiation and warm the surface; however, during the summer months when the surface snow cover disappears, clouds reduce the shortwave radiation more effectively than the increase of longwave radiation and the surface is cooled.

Compared to the observations on the sea ice at Syowa Station, Antarctica, the net total radiation at Ny-Ålesund is much larger in the summer months than at Syowa Station. These are the results of lower albedo in summer months, larger downward radiation due to warmer temperatures and clouds. As a whole, the radiation budget at Ny-Ålesund in summer is controlled by the maritime airmass, while in winter it is strongly affected by both maritime air from the south and Arctic air from the north.

1. Introduction

The radiation budget is one of the most important components of the climate in the Arctic, and then interfere the role of the Arctic in the global climate. Most of the Arctic is composed of the Arctic Ocean, which is covered with sea ice the whole year around. The Svalbard islands are located at the edge of the seasonal ice cover, mostly surrounded by drift ice in late winter but by open water in other seasons. Svalbard is located in the middle of an active atmospheric and oceanic transport zone; most of the ice produced

in the Arctic Ocean flows out through the Fram Strait west of Svalbard, and the frequency of cyclone passage is high.

The National Institute of Polar Research, Japan, has started a manned and unmanned observatory at Ny-Ålesund, Svalbard, since the establishment of the Arctic Environment Research Center. The surface radiation budget has been measured for a long time since 1974 at the Norwegian Polar Institute Research Station in Ny-Ålesund. Some data are reported year by year (VINJE, 1975–80) and some have been published as a data report (HISDAL et al., 1992). A short description of general characteristics of the radiation budget has already been given by VINJE (1975). Recently, the Alfred Wegener Institute, Germany, has also started surface radiation measurements at Ny-Ålesund. The measurements are part of the BSRN (Baseline Surface Radiation Network; WMO, 1991), maintained in cooperation with the Norwegian Polar Institute.

The present paper discusses the radiation climatology at Ny-Ålesund during 1987, based on data measured by the Norwegian Polar Institute (HISDAL et al., 1992). The shortwave and longwave radiation fluxes are discussed with daily mean values, and compared to those at Syowa Station, Antarctica, for the purpose of studying the characteristics of the radiation budget in the Arctic.

2. Data

Data of radiation fluxes are derived from the report by HISDAL et al. (1992). The surface radiation fluxes have been measured at Ny-Ålesund (78°55′ N, 11°56′ E) on the west coast of Spitsbergen since 1974 (Fig. 1). Since 1981, upward looking sensors have
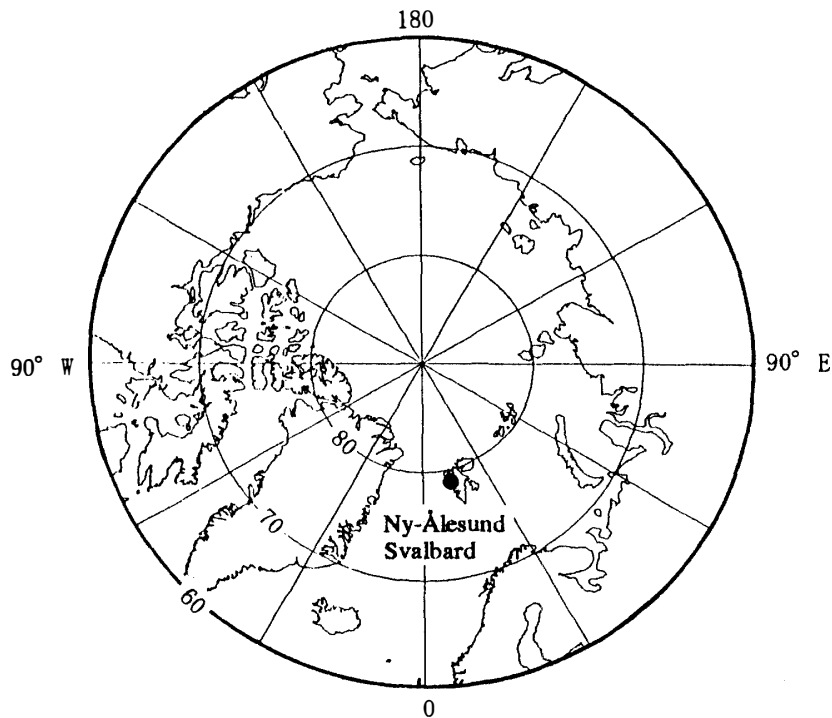

Fig. 1. Location map of Ny-Ålesund, Svalbard in the Arctic.

been mounted on the roof of the station building (17 m a.s.l.) and down facing and net instruments on the tundra nearby (12 m a.s.l.). The horizontal view is limited by mountains; Zeppelinfjellet to the south reaches an elevation of $13.7°$, and Scheteligfjellet to the west reaches $8.4°$ of the horizon. The polar night starts and ends on October 25 and February 17, respectively, while the period with midnight sun lasts from April 28 to August 17.

The global solar radiation was measured by Eppley pyranometers, calibrated temporally with an Ångstrom pyrheliometer. The reflected shortwave radiation was measured by Eppley pyranometers mounted on the tundra about 1.8 m above the bare ground. With snow cover, the height above the surface could decrease to less than half of this value.

The total downward radiation was measured by a Siemen Ersking pyradiometer, with separate calibration constants for shortwave and longwave. The longwave component was calculated by subtracting shortwave from the total. Though the calibration constants were given separately, hourly downward longwave radiation data still show some unreasonable regular diurnal variation following the global radiation change in the sunlit season. These diurnal variations might be due to improper calibration constants or due to the zenith angle dependence of the shortwave calibration constant, and determine the range of uncertainty of the measurements as about ± 10 W/m^2.

Data of surface meteorological observations including air temperature at every 6 hours and cloud amount were supplied from the Norwegian Meteorological Institute.

3. Shortwave Radiation

3.1. Albedo

The variation of albedo, as seen in Fig 2, is drastic. After the sun rises above the horizon at the end of February, the albedo remains at around 80% until May. After snow melts in June, the albedo drops to the minimum of about 15%, and stays at this
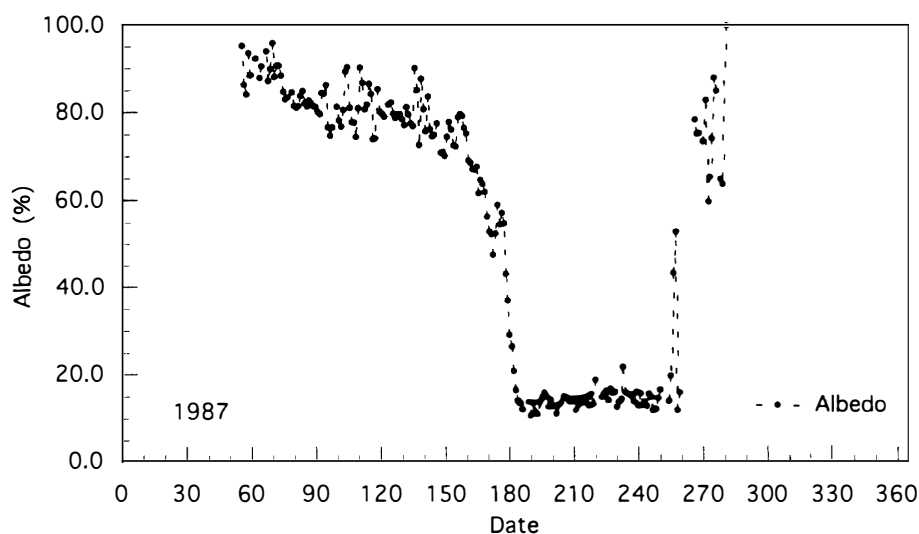

Fig. 2. Daily mean albedo at Ny-Ålesund, Svalbard in 1987. Points at 100% albedo are meaningless due to small amount of global radiation.

low value during two and half months. In the middle of October, the returning snow causes the albedo to increase and reaches the value of about 80% again. After the end of the data record, no reasonable albedo is obtainable due to low solar elevation height or no solar radiation, since the sun is below the horizon between October and February.

The variable albedo in September is due to snow showers and snow melt, before the surface is covered with a permanent snow cover. After about a month, snow cover became permanent and prevailed during winter.

3.2. Global radiation

Figure 3 shows the daily average of global solar radiation at the surface (SWD) compared to that at the top of the atmosphere (INSO). After four months of polar night, solar radiation starts to increase at the end of February, with the increasing solar elevation. The global radiation varies largely from clear sky to overcast, and from the end of May to July, the maximum values lie around 350 W/m². The global radiation decreases to zero with frequent variation in late October.

The transmittance of global solar radiation defined as the ratio of global radiation at the surface to the solar insolation at the top of the atmosphere is shown in Fig. 4. Except for the first few days when the sun is only slightly above the horizon, making the reliability low because the result is obtained as a ratio of small values, the transmittance increases in March, becomes higher in April, May and the first half of June, and varies between about 40% to 70% depending on the cloud condition. From the second half of June, the transmittance is rather smaller on average, and varies between 60% under clear sky and about 20% under cloudy sky. This variation of transmittance is not only due to the variation of the real transmittance of the atmosphere and cloud amount. The atmospheric transmittance decreases due to the increase of atmospheric water vapor amount with the temperature increase. The variation of the measured transmittance is also attributable to the variation of the surface albedo, which affects the multiple
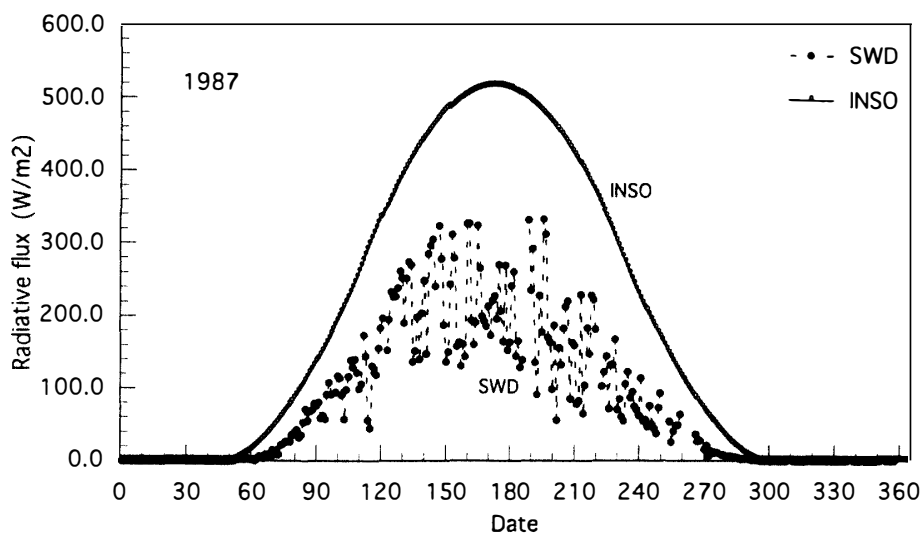

Fig. 3. Daily mean global solar radiation (SWD) at Ny-Ålesund, Svalbard in 1987, together with the solar insolation at the top of the atmosphere (INSO).
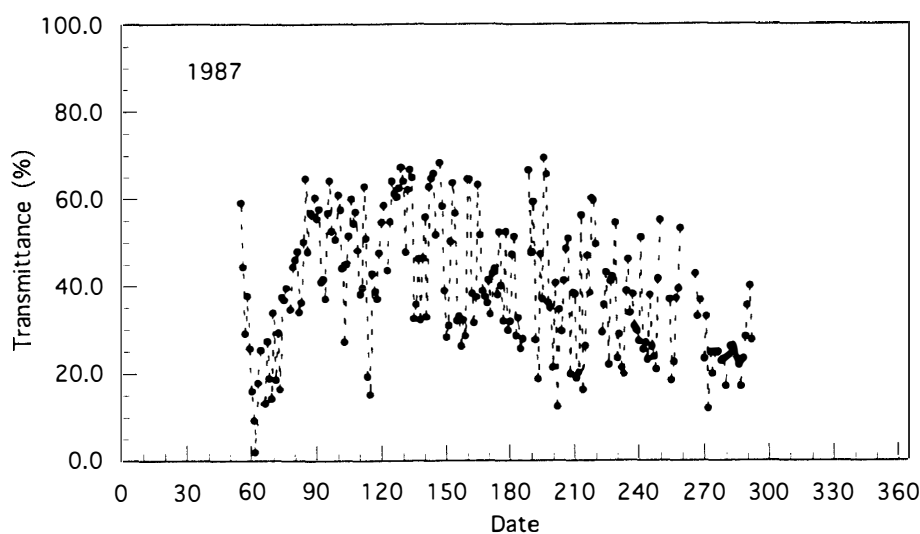
Fig. 4. *Transmittance of the global solar radiation defined as a ratio of the daily mean global radiation at the surface to the daily mean solar insolation at the top of the atmosphere, Ny-Ålesund, Svalbard, 1987.*

scattering of solar radiation between the surface and the atmosphere or clouds. Large multiple scattering with high surface albedo until June contributes to the high transmittance.

The figure is not symmetric with respect to midsummer, due to the change in surface albedo. The great decrease in the surface albedo as seen in Fig. 2 reduces the transmittance in the latter half of summer after July. Although the solar insolation at the top of the atmosphere is symmetric against day 173, the transmittance and then the global solar radiation tend to be smaller after July due to this lowering of the albedo.

4. Longwave Radiation

4.1. Downward radiation

The variation of daily mean downward longwave radiation (LWD) also has a significant change between winter and summer as shown in Fig. 5. The lower envelope drawn in the figure corresponds to longwave radiation for the clear sky. The envelope curve shows low values around 150 W/m^2 from the end of October to March, and increases between April and June. In the summer months, June, July and August, higher values of about 270 to 300 W/m^2 are evident before the curve decreases back to the lower value in October. The upper envelope curve corresponds to the extreme overcast days. It is interesting to note that this curve ranges between 300 and 350 W/m^2 and does not change greatly between winter and summer in spite of the large change in the lower envelope.

The variability of the downward longwave radiation is small in summer and large in winter. This is a great difference from the downward longwave radiation measured in Antarctica (for example at Mizuho (YAMANOUCHI and KAWAGUCHI, 1984) and Syowa (YAMANOUCHI, 1989)).

The surface temperature estimated from the upward longwave radiation as black

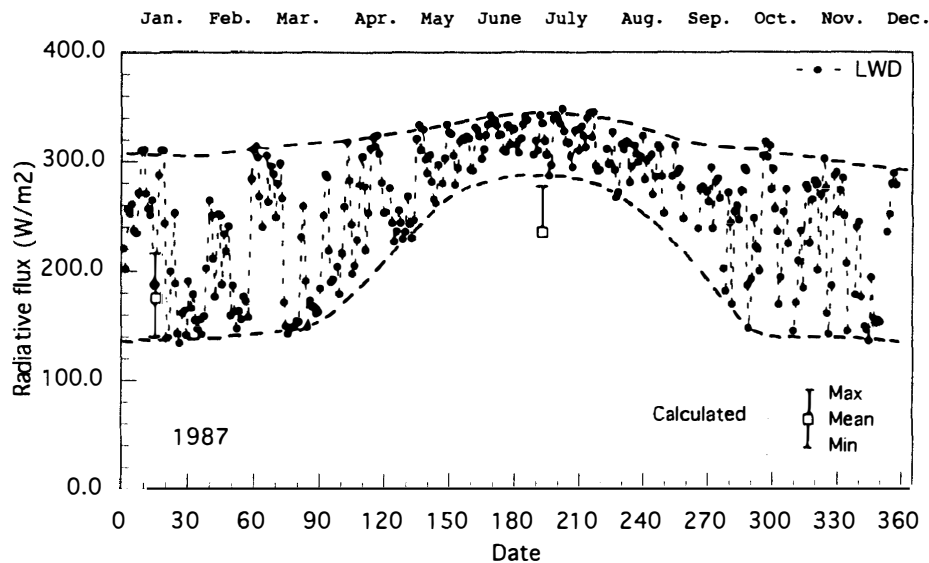Jan. Feb. Mar. Apr. May June July Aug. Sep. Oct. Nov. Dec.

Fig. 5. Daily mean downward longwave radiation at Ny-Ålesund, Svalbard in 1987. Envelopes of the maximum and minimum downward longwave radiation, and calculated mean (Mean), maximum (Max)and minimum (Min)downward longwave radiation based on the aerological data in January and July, 1992, are shown.

body radiation is higher than 0°C in summer, and it is much higher under clear than under cloudy sky. From the end of June, the higher surface temperature under the clear sky is due to the low surface albedo, which makes the reduction of solar radiation by clouds larger than the increase of downward longwave radiation by clouds. As a total, net radiation decreases by clouds and the temperature under cloudy sky becomes much lower than that under clear sky. High humidity of more than 80% most of the time in summer also increases the downward longwave radiation even under clear sky. High temperature with high humidity makes the downward radiation larger on clear days. On the other hand, under cloudy sky temperature is lower than on clear days, resulting in smaller downward longwave radiation as a cloudy condition. These factors reduce the difference of downward longwave radiation between cloudy and clear days.

The opposite effect is seen in winter, with lower atmospheric temperature and lower surface temperature under clear sky than under cloudy sky; the water vapor amount is small at temperatures as low as $-30°C$, so that the downward longwave radiation is low. With small water vapor amount, clouds are much more effective in increasing the downward longwave radiation; however, the effect of clouds alone is not enough to increase downward radiation to above 300 W/m². The large rise of air temperature causes the increase of downward longwave radiation.

4.2. Comparison with calculation

In order to clarify the above explanation, the downward longwave flux was calculated for the model atmosphere, using a simple radiation code (RAMANATHAN, 1976), giving good results compared to the measurements at Mizuho Station, Antarctica (YAMANOUCHI and KAWAGUCHI, 1984). Since there were no aerological observations

in 1987, we have used the results from 1992, with aerological observations made by AWI since 1991. The calculations were done for clear sky (no cloud) with temperature profiles based on the monthly averages in January and July, together with the extreme low or high temperature profiles, shown in Fig. 5. In January, the monthly mean calculated flux lies between the lower envelope curve for clear sky and the upper envelope curve for overcast. The calculated flux for the lower extreme temperature profile (clear day) lies close to the clear day envelope. In July, the monthly mean calculated flux lies below the clear envelope. As mentioned before, in July, the temperature under clear sky is higher than the temperature under cloudy sky. The downward flux calculated for the monthly mean temperature but with no cloud is lower than that for the clear and of course lower than that for the cloudy case, and is also lower than the measured average. The calculated flux for the higher extreme tempera- ture profile (which should correspond clear day) is higher than that for the monthly mean, and lies close to the measured envelope curve for the clear sky. Since the calculations were not done for the actual atmospheric profile, it is not necessary to have quantitative agreement; however, the calculation generally supports the explanation given above.

4.3. Climatological explanation

The principal features of Fig. 5 are now attributable to the atmospheric tempera- ture variations during winter and summer. Figure 6 shows the average winter and summer sea ice extent around Svalbard (VINJE, 1982). The figure indicates that Svalbard is within the extent of sea ice (close to the edge) in winter, but is surrounded by open water in summer. Ny-Ålesund is surrounded by maritime air in the summer, but can be covered either with maritime air from the south or the Arctic air from the northern sea ice area in winter.

Hourly mean downward longwave flux in January is shown in Fig. 7 for January 1987. Comparing the longwave flux variations with the 500 hPa Northern Hemisphere weather chart of Fig. 8 (JMA, 1987), we can clearly identify the dates January 16, 21 -23, 26, 27 and 30, on which the lowest downward flux less than 150 W/m², with cold Arctic air outflows to the east of the high pressure ridge over Greenland along the western side of Svalbard (Fig. 8a). On the other hand, days January 10, 18, 19, with the highest extreme of downward flux of more than 300 W/m², had deep depressions approaching from the southwest, leading to a transport of mild maritime air from lower latitudes (Fig. 8b). The relations of the surface temperature variation for these typical circulation patterns at Svalbard have already been explained in general by HISDAL (1975). In the first week of January, the downward longwave flux varies between about 190 to 250 W/m², and variation is smaller than in other term even with cloud amount change from 0 to 10, when the surface temperature lies around −5 °C. The weather chart (Fig. 8c) shows a circulation pattern different from both Fig. 8a and b, with a high pressure ridge near Svalbard, sparse distribution of geopotential height contours and weak winds.

Figure 9 from BARRY et al. (1993), based on SCHWEIGER and KEY (1992) and WARREN et al. (1989), shows climatological mean cloud cover in the Arctic. In summer (b), most of the Arctic including the Greenland Sea and Svalbard is covered with high
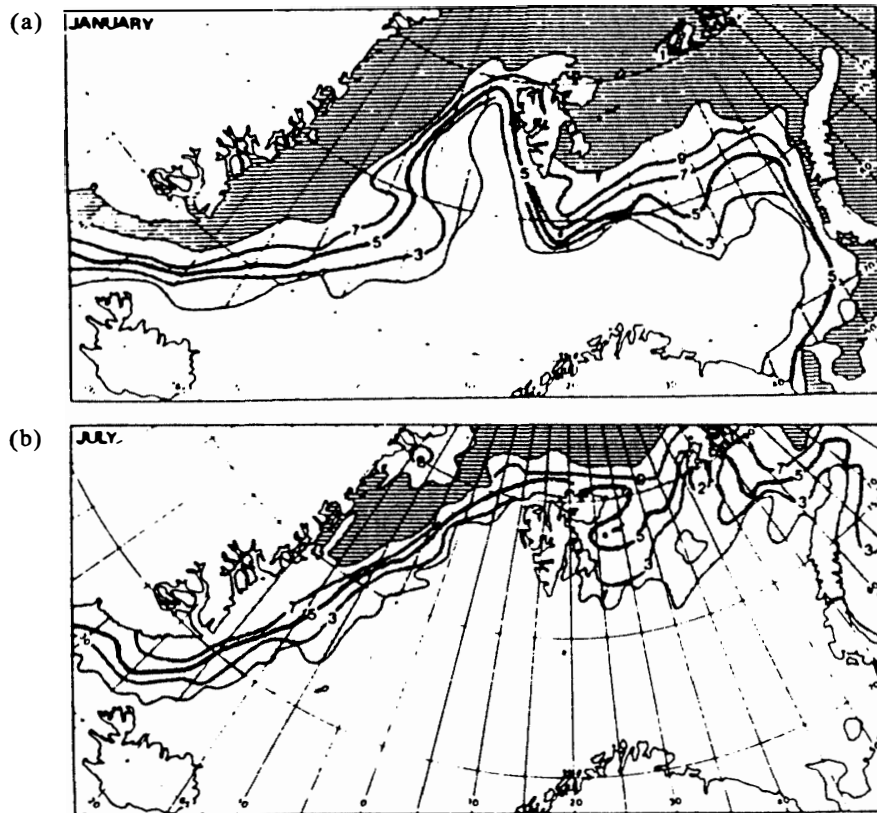
Fig. 6. *Frequency distribution (in tenths) of sea ice concentration above 4/10 at the end of (a) January and (b) July, during 1971–80. i.e. the curve marked 5 gives the southern border for ice in 5 out of 10 years (after HANSSEN-BAUER et al., 1990).*
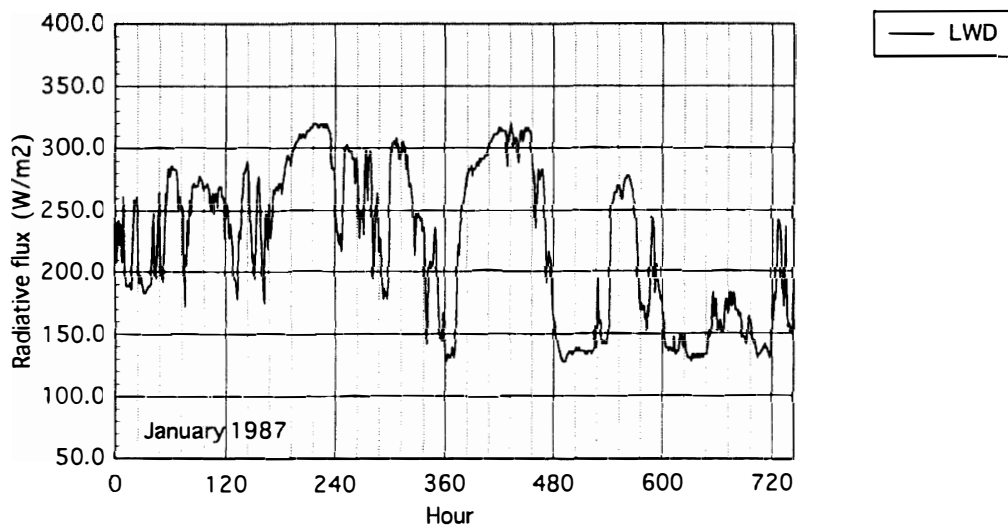

Fig. 7. *Hourly downward longwave radiation at Ny-Ålesund, Svalbard in January 1987.*

Fig. 8. 500 hPa Northern Hemisphere weather chart (JMA, 1987) on (a) January 22, (b) January 19 and (c) January 3, 1987 (number: height in 10 m).

Fig. 9. Mean cloud cover (in percent) for (a) January and (b) July, from BARRY et al. (1993), based on SCHWEIGER and KEY (1992) and WARREN et al. (1989).

cloud fraction, about 80%. In winter, however, the central part of the Arctic Sea is covered with low cloud amount, while the southern part, the Greenland Sea, is covered with high cloud amount. Svalbard is just at the border between high cloud amount region to the south and low cloud amount region to the north. It can be assumed that in winter, if Svalbard is covered with a southern air mass, then the temperature and humidity are high due to maritime air and the sky is mostly cloudy, while if Svalbard is covered with a northern Arctic airmass, then the temperature is low and likely to be

clear. Cloudy sky condition may also exist in the Arctic airmasses, in which case downward longwave fluxes and surface temperatures will be lower, corresponding to intermediate points between the two envelope curves in Fig. 5. The large variation in the winter is thus mainly caused by the alternation of different airmasses; variations in summer are smaller due to the more homogeneous airmasses.

5. Net Radiation and Comparison with Antarctic Data

The daily mean net longwave radiation is shown in Fig. 10 together with the upward and downward radiations. Even though we have large differences between summer and winter for the downward longwave radiation as seen in Fig. 5, there are no substantial differences in the net longwave radiation between summer and winter. The range of the net longwave radiation variation is about 80 W/m² throughout the year. From October to May, the upward longwave radiation increases following the increase of the downward radiation due to clouds, because the total net radiation tends to increase due to the clouds, larger absorption of radiant energy occurs and the surface temperature rises. From the end of June to August, snow cover disappears and the ground surface becomes bare rock and tundra, with a much lower surface albedo, and clouds will effectively reduce the shortwave radiation and cool the surface. However, because the heat conductivity of soil and rock is higher than snow, the surface temperature itself does not follow the net radiation so closely as in the case with snow. Figures 11a and b clearly show this relation. In winter (January) with snow cover, the surface temperature (parallel to the upward radiation) quickly follows the net radiation, and increases
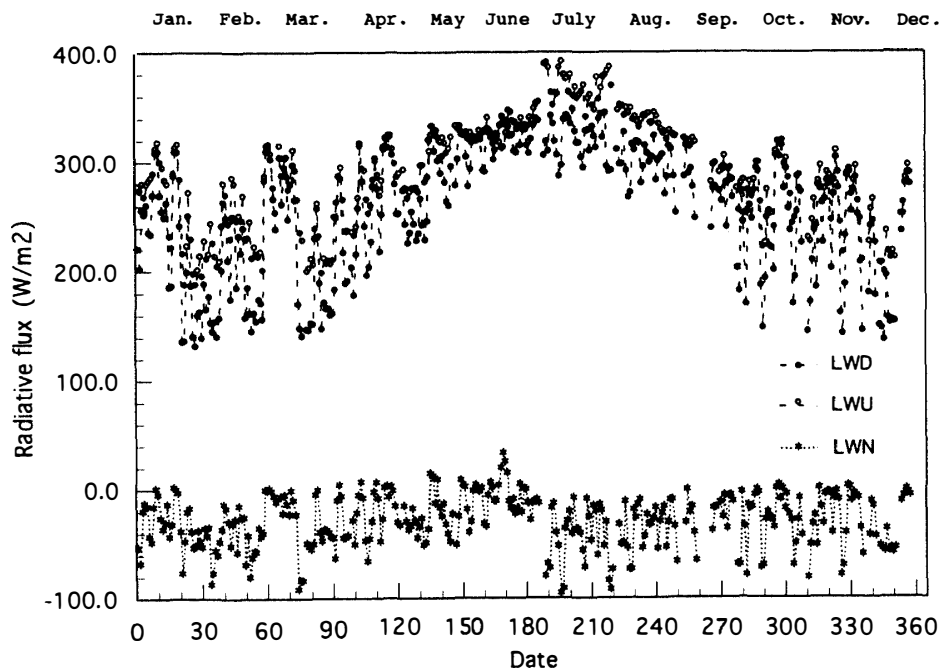

Fig. 10. Daily mean downward (LWD), upward (LWU) and net (LWN) longwave radiation at Ny-Ålesund, Svalbard in 1987.
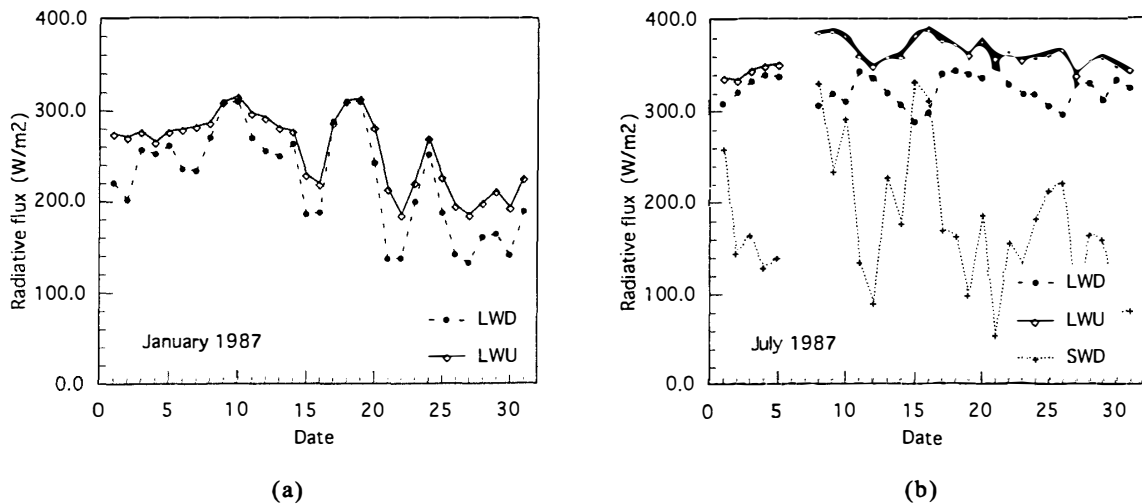
Fig. 11. Day to day variation of downward longwave (LWD), upward longwave (LWU) and global radiation
(SWD; only for July) at Ny-Ålesund, Svalbard in (a) January and (b) July, 1987.

suddenly following the increase of the downward flux due to clouds. In summer (July), the surface temperature slowly increases following the decrease of downward longwave radiation, when the shortwave downward radiation increases. The variation of the surface temperature in summer is smaller compared with the similar net radiation variation in winter.

Monthly mean components of the radiation budget, the longwave downward, longwave upward, global, and reflected shortwave radiation, for 1987 are shown in Fig. 12. The upward and downward longwave radiations in Ny-Ålesund increase from February to July and decrease to December. The difference in the upward and downward longwave radiation becomes small in June as is already seen in Fig. 10. The
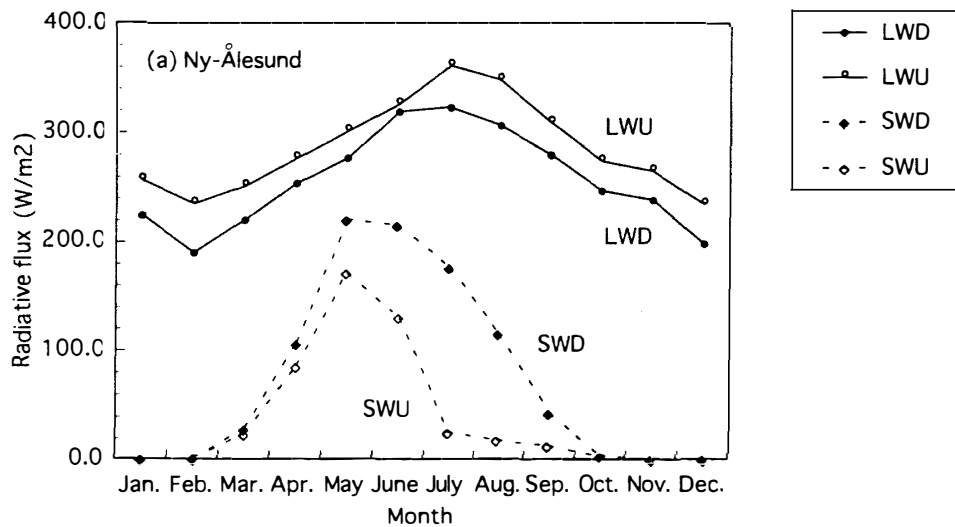

Fig. 12. Monthly mean downward shortwave (SWD), upward shortwave (SWU), downward
longwave (LWD) and upward longwave (LWU) radiation fluxes at (a)
Ny-Ålesund, Svalbard and (b) Syowa Station, Antarctica, in 1987 (88). In order
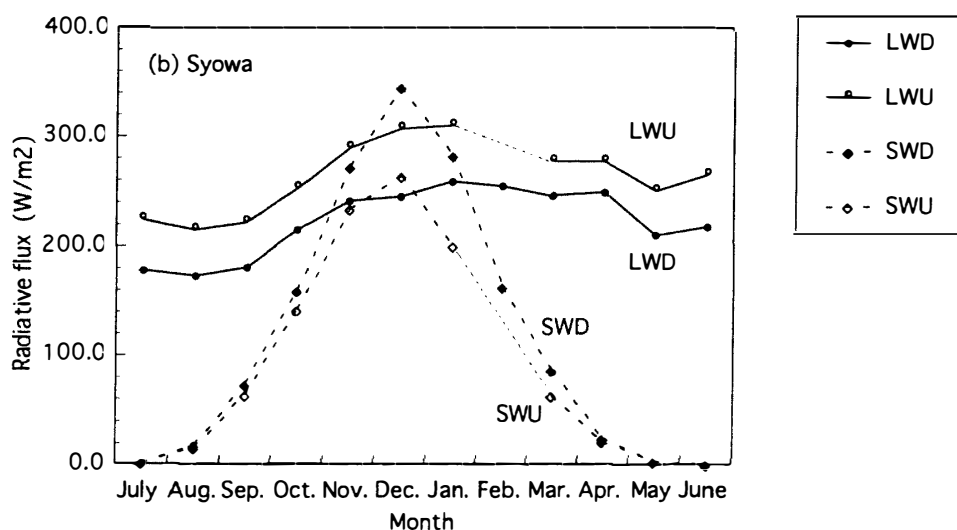to make a direct comparison, data for Syowa Station are shifted 6 months.

Fig. 12.

global radiation should increase under normal conditions from May to June due to the increase of mean solar elevation height. However, the global radiation decreases in this period, together with the difference of the longwave radiation, due to the higher cloud cover in this month. Because of the reduction in albedo, the reflected shortwave radiation starts to decrease in June and stays small until September.

Comparison is also made in Fig. 12 with the monthly mean fluxes measured at Syowa Station (69°00′ S, 39°35′ E ; YAMANOUCHI, 1989) in the same year, a typical example of a coastal station in Antarctica. The plots are shifted half a year to be comparable to the seasonal variation in the Northern Hemisphere. The shortwave radiation at Syowa has a rather symmetrical seasonal variation centered in June, and the fluxes are larger than at Ny-Ålesund due to the lower latitude and higher albedo of the surface covered with snow or sea ice. The upward and downward longwave fluxes at Ny-Ålesund are larger than those at Syowa, except for months 10 and 12 (October and December at Ny-Ålesund against April and June at Syowa). The difference in upward and downward longwave radiation at Ny-Ålesund is smallest in summer, and smaller than that at Syowa throughout the year.

Monthly mean net radiation fluxes are shown in Fig. 13, together with those at Syowa Station. Larger net shortwave radiation results in larger net total radiation at Ny-Ålesund in the summer months. The net longwave radiation at Ny-Ålesund is larger (smaller cooling) than that at Syowa in summer months, especially in June, and similar in winter months with that at Syowa.

The net total radiation in the summer months at Ny-Ålesund is much larger than that at Syowa Station; it is positive for 5 months from May to September at Ny-Ålesund, compared to only three months at Syowa. These are the results of lower albedo in the summer months from June to September, larger downward radiation and small absolute amount of net longwave radiation due to clouds.

Another comparison is made with the typical example of radiation fluxes at the central Arctic based on MAYKUT (1986) shown in Fig. 6 of BARRY et al. (1993). the seasonal variation of the downward longwave radiation in the central Arctic is much
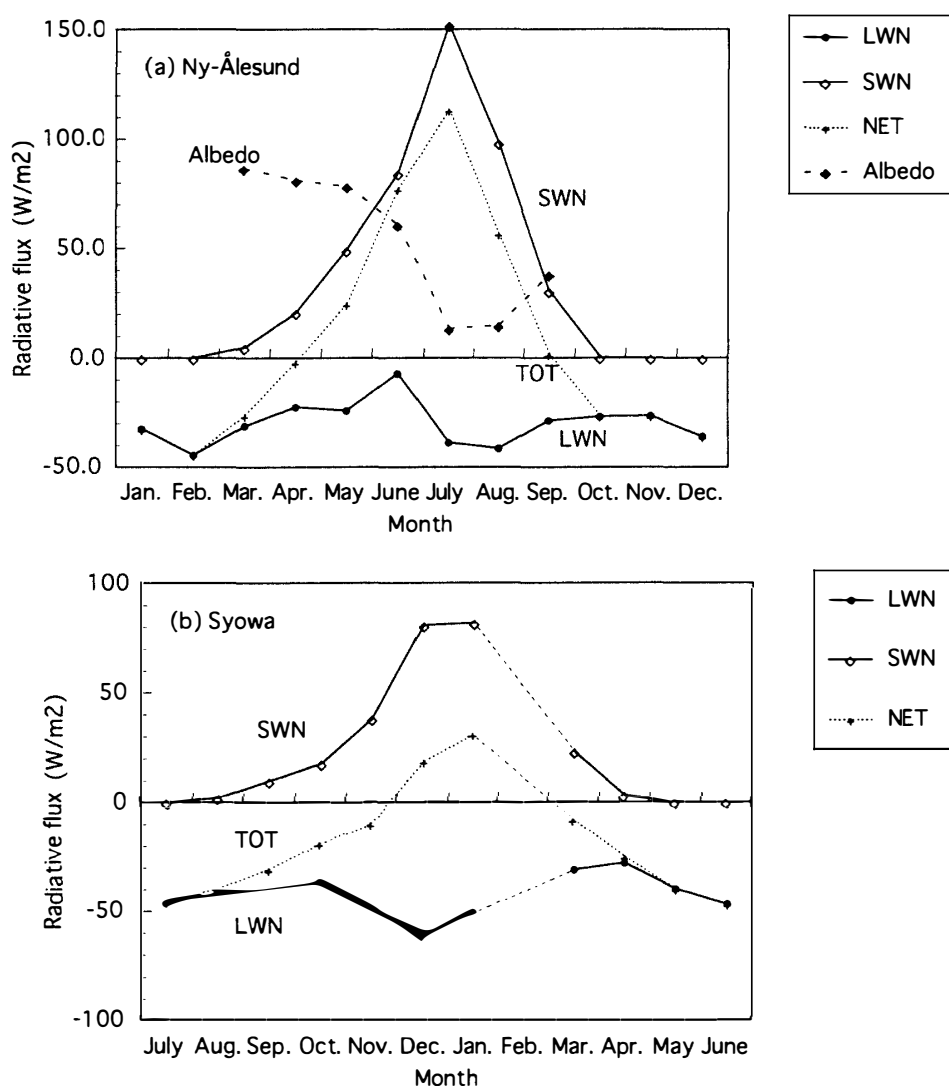
Fig. 13. Monthly mean net shortwave (SWN), longwave (LWN) and total (TOT) radiation fluxes at (a) Ny-Ålesund, Svalbard and (b) Syowa Station, Antarctica in 1987 (88). Data for Syowa Station are shifted 6 months.

similar to the lower envelope curve for clear sky as shown in Fig. 5, and much smaller than the monthly average in winter months at Ny-Ålesund, mainly due to a smaller cloud amount and lower temperatures of the central Arctic air. The global solar radiation is also much larger due to the smaller cloud amount, and the net shortwave radiation is smaller due to the higher albedo throughout the year. The total net radiation is smaller in the central Arctic basin in the summer, but still positive in the same 5 months as at Ny-Ålesund.

6. Concluding Remarks

The general characteristics of the surface radiation budget at Ny-Ålesund, Svalbard are controlled by the surface snow cover, the cloud amount and the exchange of air

masses between cold Arctic air and mild moist maritime air. The surface albedo decreases suddenly when the snow melts in June, making the apparent transmittance of the atmosphere, defined as the ratio of the global radiation to the solar insolation at the top of the atmosphere, smaller.

The downward longwave radiation shows large variability in winter due to the variation in the air masses covering Svalbard. The temperature, humidity and cloud amount change drastically with cold air from the Arctic Basin and maritime air from the lower latitude ocean areas. In these cases, it is not straightforward to define the cloud radiative forcing just by the difference in mean and clear fluxes. In summer, the downward longwave radiation shows rather small variability, due to the smaller difference in the airmass surrounding Svalbard and constant high cloud amount.

Compared to the data at Syowa Station, Antarctica, the net (total) radiation at Ny-Ålesund is much larger in the summer months, due to a lower albedo, warmer temperature, higher humidity and higher cloud amount. As a whole, the radiation budget at Ny-Ålesund is prescribed by the maritime airmass in summer, and strongly affected by both the maritime air from the south and the Arctic air from the north in winter. Though the analysis was done only for one place and for one year, the conclusion should also hold for the surrounding seasonal sea ice areas in the Arctic.

Acknowledgment

References

BARRY, R. G., SERREZE, M. C. and MASLANIK, J. A. (1993): The Arctic sea ice-climate system: Observations and modeling. Rev. Geophys., 31, 397–422

HANSSEN-BAUER, I., KRISTENSEN SOLÅS, M. and STEFFENSEN, E. L. (1990): The Climate of Spitsbergen. Det Norske Meteorologiske Institutt, Rapport, 39/90, 40 p.

HISDAL, V. (1975): The weather in Svalbard in 1974. Norsk Polarinstitutt Årbok, 1974, 195–198.

HISDAL, V., FINNEKÅSA, Ø. and VINJE, T. (1992): Radiation Measurements in Ny-Ålesund, Spitsbergen 1981–1987. Oslo, Norsk Polarinstitutt, 380 p. (Meddelelser NR 118).

JAPAN METEOROLOGICAL AGENCY (1987): Daily Weather Maps, January and July, 1987.

MAYKUT, G. A. (1986): The surface heat and mass balance. The Geophysics of Sea Ice, ed. by N. UNTERSTEINER. New York, Plenum, 395–464 (NATO ASI Series, Ser. B Phys., 146).

RAMANATHAN, V. (1976): Radiative transfer within the earth's troposphere and stratosphere: A simple radiative-convective model. J. Atmos. Sci., 33, 1330–1346.

SCHWEIGER, J. A. and KEY, J. (1992): Arctic cloudiness: Comparison of ISCCP-C2 and Nimbus-7

satellite-derived cloud products with a surface-based cloud climatology. J. Clim., **5**, 1514–1527.

VINJE, T. (1975–1980): Radiation conditions in Spitsbergen in 1974–1979. Norsk Polarinstitutt Årbok, **1974 –79**.

VINJE, T. (1982): Frequency distribution of sea ice in the Greenland and Barents Seas 1971–80. Norsk Polarinstitutt Årbok, **1980**.

WARREN, S. G., HAHN, C. J., LONDON, J., CHERVIN, R. M. and JENNE, R. L. (1989): Global Distribution of Total Cloud Cover and Cloud Type Amounts Over the Ocean. Boulder, NCAR, 150 p.

WMO (1991): Radiation and Climate, Workshop on Implementation of the Baseline Surface Radiation Network, Washington, DC, U. S. A., 3–5 December 1990. WCRP, **54**, 8 p. (WMO/TD - No. 406)

YAMANOUCHI, T. (1989): Radiation data at Syowa Station, Antarctica from February 1987 to January 1988. Antarctic Climate Research Data, part 1. JARE Data Rep., **144** (Meteorology 22), 193 p.

YAMANOUCHI, T. and KAWAGUCHI, S. (1984): Longwave radiation balance under a strong surface inversion in the katabatic wind zone, Antarctica. J. Geophys. Res., **89**, 11771–11778.